Available online at www.sciencedirect.com

ScienceDirect

Mendeleev Commun., 2023, **33**, 282–284

Mendeleev Communications

The impact of the SnI_2 purity on the formation of $CsSnI_3$ perovskite modifications as monitored by ^{127}I Nuclear Quadrupole Resonance

Eleonora A. Kravchenko,[a] Andrei A. Gippius,[b,c] Aleksei V. Tkachev,[c] Maksim V. Mastryukov[a] and Maria N. Brekhovskikh*[a]

[a] *N. S. Kurnakov Institute of General and Inorganic Chemistry, Russian Academy of Sciences, 119991 Moscow, Russian Federation. E-mail: mbrekh@igic.ras.ru*
[b] *Department of Physics, M. V. Lomonosov Moscow State University, 119991 Moscow, Russian Federation*
[c] *P. N. Lebedev Physical Institute, Russian Academy of Sciences, 119991 Moscow, Russian Federation*

DOI: 10.1016/j.mencom.2023.02.043

The relative content of the perovskite phase in two $CsSnI_3$ samples (of 99.900 and 99.999 wt% SnI_2 and 99.999 wt% CsI purity) was estimated using ^{127}I NQR. The results showed that both samples contained the non-perovskite orthorhombic phase as an admixture. In the sample of higher purity (99.999 wt%) its content was insignificant – only trace amounts could be observed at 77 K, whereas at room temperature the presence of the non-perovskite phase was not revealed. However, in the sample of 99.900 wt% purity the content of the non-perovskite phase has reached at least a third of the sample amount, which is due to the probable crystallization of the non-perovskite phase on impurities.

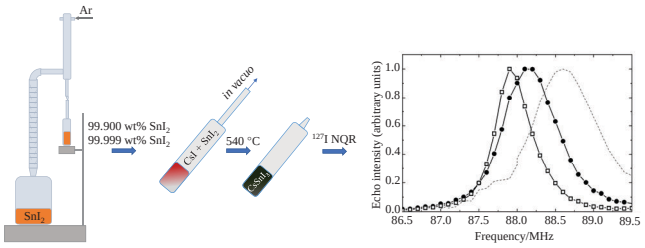

Keywords: nuclear quadrupole resonance, impurities, perovskites, purification, tin iodide.

The development of technologies for the manufacture of solar cells based on compounds with the perovskite structure requires careful control of the purity of the initial materials. The purity of the raw materials determines the characteristics of the solar cell. Thus, it was found that changing the purity of PbI_2 from 98 to 99.9% significantly affects the degree of crystallinity and grain size of $MAPbI_3$ (MA = methylammonium) and ultimately affects the efficiency of the solar cell.[1] Solar cell synthesized from MAI and PbI_2 with 99.9 wt% purity achieved a maximum efficiency up to 12.6% compared with an efficiency value of 4.9% revealed for a cell with PbI_2 of 98 wt% purity.[1]

It was shown that for a solar cell with $MAPbI_3$ as a light absorbing layer an increase of iron impurity (in the form of FeI_2) concentration by more than 10 ppm significantly reduced the efficiency of the device.[2] The impurities in the initial components were found to reduce the crystallinity of the film, the lifetime of charge carriers, the diffusion length as well as the photoelectric characteristics.[3–5] The use of high purity precursors (PbI_2, 99.999%) makes it possible to achieve an efficiency value of 16.4%. The efficiency of perovskite solar cell (PSC) with $MAPbI_3$ synthesized from extra pure grade PbI_2 is 30–40% higher than that of PSC synthesized from raw substance. The photovoltaic characteristics of the PSC depend to a large extent on the morphology of the perovskite layer that is sensitive to the conditions of the perovskite synthesis. The technique for perovskite films deposition was optimized, this resulted in changing the crystallization temperature of the perovskite films and the composition of the hole conducting layer.[6–8] However, there are no data on the effect of the purity of the SnI_2 precursor on the physicochemical properties of the perovskite $CsSnI_3$. Three (B) perovskite polymorphs of black color are known to exist: B-α $CsSnI_3$,[9,10] B-β $CsSnI_3$[11] and B-γ $CsSnI_3$.[11,12] Herewith, the last two of them are similar to B-α $CsSnI_3$ phase but they are characterized by different extent of the $\{SnI_6\}$ octahedra distortion. These phases exist at different temperatures: cubic B-α $CsSnI_3$ at above 150 °C and orthorhombic B-γ $CsSnI_3$ at temperatures below 89 °C. Thus, B-γ $CsSnI_3$ phase appeared to be the most suitable for photovoltaic applications.[12] A non-perovskite one-dimensional yellow (Y) phase is known as well. Eventually, any modification of $CsSnI_3$ transforms into Cs_2SnI_6 in the air.[13,14]

Hence, the aim of this work was to explore the effect of the SnI_2 purity on the formation of $CsSnI_3$ perovskite modifications. For this purpose, two samples of $CsSnI_3$ of different initial SnI_2 purity (99.900 and 99.999 wt%) were studied by nuclear quadrupole resonance (^{127}I NQR).

The $CsSnI_3$ perovskite synthesis was conducted for 6 h *via* the interaction of SnI_2 of different purity (99.900 and 99.999 wt%) with CsI (99.999 wt%) in a sealed evacuated quartz ampoule at 540 °C followed by cooling the ampoule with perovskite to 25 °C for 2 h. The initial SnI_2 was synthesized by the reaction of elementary Sn and I_2 in a sealed evacuated three-compartment quartz ampoule and purified by high temperature fractional distillation in a plate column.[15] After reaching about 349 °C (boiling point of SnI_4), the low-boiling fraction of SnI_4 and the high-boiling fraction of SnI_2 (bp 714 °C) were separated in a rectification column. We used SnI_2 of 99.9 wt% purity from the head fraction of the rectification process. It contained such main impurities as iron, cadmium and nickel iodides, their boiling points were close to that of SnI_2. SnI_2 of 99.999 wt% purity from

Table 1 The ^{127}I NQR spectra of $CsSnI_3$.

Compound	*T*/K	ν_1/MHz	ν_2/MHz	e^2Qq/h/MHz	η	Assignment
$CsSnI_3$(G)[a]	77	25.30	43.10	147.5	0.376	I (3)
Non-perovskite orthorhombic[26]		58.25	99.50	340.4	0.373	I (2)
		81.29	138.70	474.5	0.374	I (1)
	293	56.86	97.42	333.1	0.369	I (2)
		79.59	137.64	469.8	0.356	I (1)
$CsSnI_3$(B)[a]	77	88.6		591	0 (assumed)	I (4)
perovskite tetragonal[26]		94.2		628	0 (assumed)	I (4)
	293	88.2		588	0 (assumed)	I (4)
		90.5		603	0 (assumed)	I (4)
$CsSnI_3$(B)[b]	77	88.15(8)		587.52(53)	0.01 (assumed)	I (4)
99.900%		93.80(8)		624.75(51)	0.03 (assumed)	I (4)
	295	87.80(7)	175.55(13)	585.19(37)	0.01 (2)	I (4)
		90.05(8)	179.90(8)	599.77(24)	0.03 (3)	I (4)
$CsSnI_3$(B)[b]	77	87.90(7)		585.86(47)	0.01 (assumed)	I (4)
99.999%		93.65(7)		623.90(44)	0.03 (assumed)	I (4)
	295	87.60(6)	175.15(12)	583.86(34)	0.01 (2)	I (4)
		89.80(7)	179.45(9)	598.25(26)	0.03 (2)	I (4)

[a] The ^{127}I NQR spectra of $CsSnI_3$ were studied at 77 and 293 K by Yamada *et al.*[26] [b] Our data for the perovskite phase.

the major fraction of rectification was used as the content of impurities in it was much lower than in the head fraction.

Impurities composition of the initial tin^{II} iodide and cesium iodide obtained in[16] was determined by inductively coupled plasma–atomic emission spectroscopy using a Thermo iCAP 6300 Duo spectrometer.

NQR is the direct, sensitive and accurate method for measuring the quadrupole interactions, the spin Hamiltonian being completely determined within the crystal field. The NQR spectroscopy deals with the electric field gradient (EFG) produced by the spatial distribution of electron density around the studied nucleus.

$$\text{EFG} = q_{ik} = -\partial E_i/\partial x_k = -\partial^2 U/\partial x_i\,\partial x_k,$$

where E_i is the strength and U is the potential of the field at the nuclear site.

This makes NQR highly sensitive to the fine details of electronic and geometric structure and crystal chemistry.[17,18] The spectroscopic parameters measured by NQR include the quadrupole coupling constant (QCC = e^2Qq_{zz}/h), the EFG asymmetry parameter ($\eta = |q_{xx} - q_{yy}|/q_{zz}$), the resonance line width ($\Delta\nu$), spin–lattice (T_1) and spin–spin (T_2) relaxation times.[17]

The main contribution to the resonance line width ($\Delta\nu$) is due to the statistical distribution of the EFG components over the sample volume because of inhomogeneity of the crystal lattice. The NQR spectra of inorganic compounds, which are mostly polymers and very rarely form molecular crystals, possess line widths of 30–50 kHz owing to the presence of impurities, dislocations, vacancies and other defects in their lattice. Very often inorganic polymers contain irremovable elements of disorder. The NQR spectroscopy was earlier used to analyze the behavior of impurities as well as the effect of particle size and density of matter on the quadrupole interaction parameters; and the NQR line width was recognized as a sensitive criterion of the crystal quality.[19,20] The method has shown high efficiency in the study of Sn- and Pb-based hybrid perovskites.[21,22]

In our previous report, the ^{35}Cl NQR spectroscopy was used to control the comparative purity of the $SnCl_4$ samples subjected to successive stages of deep purification.[23]

As would be expected, fractional distillation ensures a fairly effective removal of the most impurities. The impurities behavior in the SnI_2 purification process is similar to the behavior of impurities in tin chlorides.[24] Difficult-to-remove impurities appeared to be Cd, Pb, Co and Fe as their iodides boiling points are close to that of SnI_2, but they were successfully removed during the purification process.[15]

Two samples of $CsSnI_3$ obtained from SnI_2 of 99.900 and 99.999 wt% purity were studied using ^{127}I NQR. As mentioned above, $CsSnI_3$ has been found in various modifications at different temperatures: perovskite phases exist as cubic (B-α)[9] at temperatures above 150 °C, tetragonal (B-β)[11] and orthorhombic (B-γ)[13] phases – at temperatures below 89 °C. A non-perovskite orthorhombic (Y) phase[25] was revealed as well.

The ^{127}I NQR spectra of $CsSnI_3$ were measured at 77 K and 293 K by Yamada *et al.*[26] (see Table 1). Two phases, perovskite B-β tetragonal and non-perovskite orthorhombic, were found to coexist in the sample at these temperatures.[26] However, the authors[26] failed to determine the ^{127}I transition frequencies for ν_2 ($\Delta m = \pm 3/2 - \pm 5/2$) for perovskite phase. Accordingly, the values of the quadrupole coupling constants (e^2Qq/h) and the EFG asymmetry parameters (η) were not defined (the values of e^2Qq/h in Table 1 were estimated assuming zero EFG asymmetry parameter).

Our samples, as evidenced by their ^{127}I NQR spectra,[†] contained both a perovskite B-β tetragonal phase and a non-perovskite orthorhombic phase. We succeeded in measuring the complete ^{127}I NQR spectra of the perovskite B-β tetragonal phase at a room temperature (see Table 1).

According to the earlier publications,[26,27] the structure of the non-perovskite $CsSnI_3$ phase consists of the distorted octahedra (SnI_6) forming double chains, so that the iodine atoms occupy three crystallographically nonequivalent positions, one edge and two bridging (two- and three-coordinated). They are designated in Table 1 as I (3), I (2) and I (1), respectively.[26] The crystals of the perovskite phase contain the linear I–Sn–I chains, the tin atoms being in a distorted octahedral environment that approaches the regular one with increasing temperature.[26] The iodine positions in the NQR spectra of the tetragonal distorted perovskite phase are denoted as I (4) (see Table 1).

Figure 1 presents the recordings of the ^{127}I NQR lines assigned to the ν_1 transitions in the spectra of two $CsSnI_3$ samples of different purity at 77 K and at room temperature. As one can see, both samples are two-phase. In the sample of 99.900% purity the content of the non-perovskite phase, considering the

[†] The ^{127}I NQR spectra were measured at room temperature and 77 K. The nuclear resonance signal was recorded by the standard Hahn spin echo technique with summation over the number of scan accumulations.

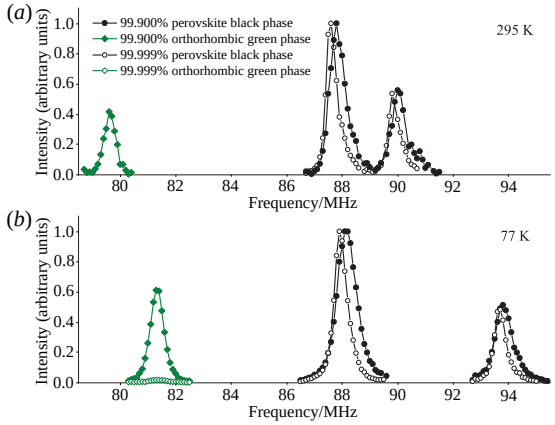

Figure 1 ^{127}I NQR lines of ν_1 transitions in the spectra of two $CsSnI_3$ samples of different purity measured (*a*) at room temperature and (*b*) at 77 K.

resonances intensity ratio, reaches at least a third of the sample amount. In the sample of 99.999% purity the content of the non-perovskite phase significantly decreases (only trace amount was observed at 77 K) while at room temperature the lines of the non-perovskite phase were not detected at all, this is due to the attenuation of the spectrometer sensitivity with increasing temperature. At the temperature rise, like in the earlier work,[26] we observed a significant convergence of the ν_1 frequencies assigned to the perovskite phase. This indicated that the structure was approaching a perovskite cubic phase with regular octahedra and a single crystallographic position of iodine atoms.

Besides the expected narrowing of the lines with an increase in the purity degree of the sample (see Figure 2), which points to the crystal perfection enhancement, we detected lowering the NQR frequencies and, accordingly, decreasing the quadrupole coupling constants value (^{127}I e^2Qq/h). At the same time, the values of the asymmetry parameters (η) remained unchanged (see Table 1). This may be due to the sharp reduction of the amount of the second (non-perovskite) phase in the sample, which is reflected in a certain strengthening of the I–Sn–I bonds (a decrease in the effective negative charge on the iodine atom) that accompanied perfection enhancement of the perovskite crystal lattice.

In conclusion, it was shown that both samples of $CsSnI_3$ of different SnI_2 purity contained the non-perovskite orthorhombic phase as an admixture. However, in the sample of the higher purity of the initial SnI_2 (99.999 wt%) the content of the non-perovskite phase was either insignificant – only trace amounts could be observed at 77 K, or it was not detected at all at room temperature. In contrast, the content of the non-perovskite phase in the sample of 99.900 wt% SnI_2 purity reached no less than one third of the sample amount on account of the probable crystallization of the non-perovskite phase on impurities.

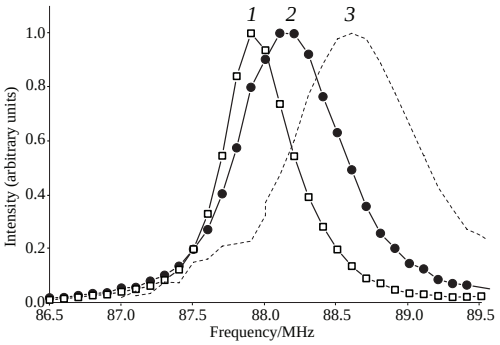

Figure 2 ^{127}I NQR lines of ν_1 transitions [site I (1)] at 77 K in the spectra of tetragonal (black) phase of the $CsSnI_3$ samples of (*1*) 99.999% SnI_2, (*2*) 99.900% SnI_2 purity degree and (*3*) published by Yamada *et.al.*[26]

This work was supported by the Ministry of Science and Higher Education of the Russian Federation as part of the State Assignment of N. S. Kurnakov Institute of General and Inorganic Chemistry of the Russian Academy of Sciences and P. N. Lebedev Physical Institute of the Russian Academy of Sciences.

References

1 J. Yao, L. Yang, F. Cai, Y. Yan, R. S. Gurney, D. Liu and T. Wang, *Sustainable Energy Fuels*, 2018, **2**, 436.
2 J. R. Poindexter, R. L. Z. Hoye, L. Nienhaus, R. C. Kurchin, A. E. Morishige, E. E. Looney, A. Osherov, J.-P. Correa-Baena, B. Lai, V. Bulović, V. Stevanović, M. G. Bawendi and T. Buonassisi, *ACS Nano*, 2017, **11**, 7101.
3 J. Chang, H. Zhu, B. Li, F. H. Isikgor, Y. Hao, Q. Xu and J. Ouyang, *J. Mater. Chem. A*, 2016, **4**, 887.
4 D. V. Amasev, S. R. Saitov, V. G. Mikhalevich, A. R. Tameev and A. G. Kazanskii, *Mendeleev Commun.*, 2021, **31**, 469.
5 D. V. Khudyakov, D. V. Ganin, A. D. Lyashedko, L. A. Frolova, P. A. Troshin and A. S. Lobach, *Mendeleev Commun.*, 2021, **31**, 456.
6 G. E. Eperon, V. M. Burlakov, P. Docampo, A. Goriely and H. J. Snaith, *Adv. Funct. Mater.*, 2014, **24**, 151.
7 S. T. Williams, F. Zuo, C.-C. Chueh, C.-Y. Liao, P.-W. Liang and A. K.-Y. Jen, *ACS Nano*, 2014, **8**, 10640.
8 A. Dualeh, N. Tétreault, T. Moehl, P. Gao, M. K. Nazeeruddin and M. Grätzel, *Adv. Funct. Mater.*, 2014, **24**, 3250.
9 C. Li, X. Lu, W. Ding, L. Feng, Y. Gao and Z. Guo, *Acta Crystallogr., Sect. B: Struct. Sci.*, 2008, **64**, 702.
10 C. Yu, Y. Ren, Z. Chen and K. Shum, *J. Appl. Phys.*, 2013, **114**, 163505.
11 W. Li, P. Liu, F. Wang, L. Pan, H. Guo, Y. Chen and S.-E. Yang, *Appl. Phys. Express*, 2020, **13**, 071003.
12 T. Ye, X. Wang, K. Wang, S. Ma, D. Yang, Y. Hou, J. Yoon, K. Wang and S. Priya, *ACS Energy Lett.*, 2021, **6**, 1480.
13 I. Chung, J.-H Song, J. Im, J. Androulakis, C. D. Malliakas, H. Li, A. J. Freeman, J. T. Kenney and M. G. Kanatzidis, *J. Am. Chem. Soc.*, 2012, **134**, 8579.
14 C. C. Stoumpos, C. D. Malliakas, and M. G. Kanatzidis, *Inorg. Chem.*, 2013, **52**, 9019.
15 M. N. Brekhovskikh, M. V. Mastryukov, P. V. Kornev, A. A. Gasanov, A. E. Kovalenko and V. A. Fedorov, *Inorg. Mater.*, 2019, **55**, 974 (*Neorg. Mater.*, 2019, **55**, 1029).
16 M. V. Mastryukov, M. N. Brekhovskikh, V. M. Klimova, P. V. Kornev and V. A. Fedorov, *Inorg. Mater*., 2020, **56**, 1050 (*Neorg. Mater.*, 2020, **56**, 1107).
17 Yu. A. Buslaev, E. A. Kravčenko and L. Kolditz, *Coord. Chem. Rev.*, 1987, **82**, 9.
18 E. A. Kravchenko, N. T. Kuznetsov and V. M. Novotortsev, *Yadernyi kvadrupol'nyi rezonans v koordinatsionnoi khimii (Nuclear Quadrupole Resonance in Coordination Chemistry)*, Krasand, Moscow, 2013 (in Russian).
19 M. L. Buess and S. M. Caulder, *Appl. Magn. Reson*., 2004, **25**, 383.
20 J. K. Jung, Y. M. Seo and S. H. Choh, *J. Chem. Phys*., 1999, **110**, 3913.
21 K. Yamada, S. Hino, S. Hirose, Y. Yamane, I. Turkevych, T. Urano, H. Tomiyasu, H. Yamagishi and S. Aramaki, *Bull. Chem. Soc. Jpn.*, 2018, **91**, 1196.
22 K. Yamada, K. Fujise, S. Hino, Y. Yamane and T. Nakagama, *Chem. Lett.*, 2019, **48**, 749.
23 E. A. Kravchenko, A. A. Gippius, A. V. Tkachev, M. V. Mastryukov and M. N. Brekhovskikh, *Mendeleev Commun.*, 2022, **32**, 567.
24 M. V. Mastryukov, M. N. Brekhovskikh, L. I. Demina, L. V. Moiseeva and V. A. Fedorov, *Inorg. Mater.*, 2022, **58**, 177 (*Neorg. Mater*., 2022, **58**, 186).
25 A. G. Kontos, A. Kaltzoglou, E. Siranidi, D. Palles, G. K. Angeli, M. K. Arfanis, V. Psycharis, Y. S. Raptis, E. I. Kamitsos, P. N. Trikalitis, C. C. Stoumpos, M. G. Kanatzidis and P. Falaras, *Inorg. Chem.*, 2017, **56**, 84.
26 K. Yamada, T. Matsui, T. Tsuritani, T. Okuda and S. Ichiba, *Z. Naturforsch., A: Phys. Sci.*, 1990, **45**, 307.
27 K. Yamada, S. Funabiki, H. Horimoto, T. Matsui, T. Okuda and S. Ichiba, *Chem. Lett*., 1991, **20**, 801.

Received: 16th November 2022; Com. 22/7043